10-2016

Comparative Study of Tumor Targeting and Biodistribution of pH (Low) Insertion Peptides (pHLIP® Peptides) Conjugated with Different Fluorescent Dyes

Ramona Cosmina Adochite
University of Rhode Island

Anna Moshnikova
University of Rhode Island, a_moshnikova@uri.edu

Jovana Golijanin
University of Rhode Island, jgolijanin@uri.edu

Oleg A. Andreev
University of Rhode Island, andreev@uri.edu

Natallia Katenka
University of Rhode Island, nkatenka@uri.edu

See next page for additional authors

Citation/Publisher Attribution

Adochite, RC., Moshnikova, A., Golijanin, J. et al. Mol Imaging Biol (2016) 18: 686. https://doi.org/10.1007/s11307-016-0949-6
Available at: http://dx.doi.org/10.1007/s11307-016-0949-6

Comparative Study of Tumor Targeting and Biodistribution of pH (Low) Insertion Peptides (pHLIP® Peptides) Conjugated with Different Fluorescent Dyes

Authors

Ramona Cosmina Adochite, Anna Moshnikova, Jovana Golijanin, Oleg A. Andreev, Natallia Katenka, and Yana Reshetnyak

Comparative study of tumor targeting and biodistribution of pH (Low) Insertion Peptides (pHLIP® peptides) conjugated with different fluorescent dyes

Ramona-Cosmina Adochite[1], Anna Moshnikova[1], Jovana Golijanin[1], Oleg A. Andreev[1], Natallia V. Katenka[2], Yana K. Reshetnyak[1,]*

[1]Physics Department, University of Rhode Island, 2 Lippitt Road, Kingston, RI 02881 USA

[2]Department of Computer Sciences and Statistics, 9 Greenhouse Road, Kingston, RI 02881 USA

Running title: Tumor targeting by fluorescent pHLIP® peptides

***Corresponding Author**: Yana K. Reshetnyak, E-mail: reshetnyak@uri.edu; Phone: 401-874-2054; Fax: 401-874-2380

ABSTRACT

Purpose. An enhanced use of glycolysis and production of carbonic and lactic acids, actively contribute to the extracellular acidosis, promoting tumor development, progression and invasiveness. pH (Low) Insertion Peptides (pHLIP® peptides) pertain to the class of pH-sensitive agents able of sensing pH at the cellular surface and delivery of imaging and/or therapeutic agents to the cancer cells in tumors.

Procedures. We investigated targeting of highly metastatic 4T1 mammary carcinoma and biodistribution of different pHLIP® variants conjugated with various fluorescent dyes. To reveal similarities and differences between investigated constructs and to identify the best pHLIP® peptide based constructs for clinical applications we employed a statistical hierarchical clustering and multivariate linear regression analyses.

Results. The highest tumor targeting with low accumulation in liver, kidney and muscle was observed for Alexa546-Var3, which also targets ~500 μm sized metastatic lesions in lungs.

Conclusions. Fluorescent pHLIP® peptides could be used for diagnostic and treatment (surgical resection) of primary tumors and submillimeter metastatic lesions.

KEYWORDS: Imaging, tumor acidity, fluorescent-guided surgery, targeting of submillimeter metastatic lesions

INTRODUCTION

A common specific feature of tumor microenvironment is a hypoxia and an extracellular acidosis [1]. The acidification of extracellular space leads to reverse of a pH transmembrane gradient in cancer cells [2-3]. Previous research showed that the acidic extracellular pH, promotes invasion and metastasis of cancer cells [4-5]. The highly proliferative cancer cells (metabolically active cells) are the most acidic. Thus, targeting of tumor acidity might be developed as an important predictive clinical marker of tumor aggressiveness and invasiveness. However, a sharp proton concentration gradient exists near the surface of cancer cells. Thus, the best approach will be to access acidity in close proximity to cancer cells in tumors.

We have introduced family of pH Low Insertion Peptides (pHLIP® peptides), which represents a unique class of water-soluble membrane polypeptides capable to undergo a pH-dependent membrane-associated folding [6-7]. pHLIP® peptides possess dual delivery capabilities, making use of the energy of folding to translocate polar cargo molecules across phospholipid bilayer of membrane and/or tether molecules to the cell surface [8]. Also, the process of peptide folding within a membrane ensures a high cooperativity of the transition, which cannot be achieved by simple diffusion [9-11]. Since pHLIP® peptides are in equilibrium between membrane-bound and non-bound configurations at normal pH they are capable of sensing pH at the cell surface. As soon as pH drops (even on a half of pH unit), the Asp and Glu residues are protonated enhancing affinity of peptides to membrane, which triggers folding in membrane and release of energy. Depending on pHLIP® sequence protonatable residues could be differently located on membrane surface, which directly affects the rate of the protonation events at various pHs, and thus pK of peptides insertion into the membrane. We have introduced family of pHLIP® peptides

with pK of insertion varying from 4.5 to 6.5 and confirmed that tumor targeting is indeed pH-dependent [9]. Three pHLIP® variants, WT, Var3 and Va7 were selected as lead candidates for pH-specific delivery of imaging and therapeutic agents to tumors of different origins. We showed previously targeting of tumors by fluorescently-labeled WT-, Var3- and Var7 pHLIP® peptides as well by the pHLIP-Fluorescence Insertion REporter (pHLIP®-FIRE) [9, 12-14]. One of the very attractive potential clinical applications of fluorescent pHLIP® peptides might be a fluorescence-guided surgical resection of tumors. The proliferative cancer cells will light up most of all targeted by the fluorescent pHLIP® agents. However, in addition to the peptide sequence variation, fluorescent dyes (which are usually about one third of pHLIP® peptides mass) can affect and alter tumor targeting and biodistribution of pHLIP® compounds. In the present study, we compared targeting of mammary tumors and biodistribution of different pHLIP® variants conjugated with eight fluorescent dyes with the main purpose to identify the best pHLIP® constructs for various clinical uses. Also, we demonstrated staining of sub-millimeter metastatic lesions in lungs by Alexa546-Var3.

MATERIALS AND METHODS

Conjugation of pHLIP® peptides with fluorescent dyes

pHLIP® variants were prepared by solid-phase peptide synthesis using Fmoc (9-fluorenylmethyloxycarbonyl) chemistry and purified by reverse phase chromatography by CS Bio. pHLIP® variants were conjugated with Alexa546-, Alexa647-, Alexa750-, Cy5.5-, DyL680-, DyL680-4xPEG-maleimide (Life Technologies) and IR680-, IR800-maleimide (LiCor Biosciences) in DMF (dimethylformamide) at a ratio of 1:1 and incubated at room temperature for about 8 hours and then at 4ºC until the conjugation was completed. The reaction progress and

purity was monitored by reverse phase HPLC to ensure absence of free dyes in the final solution. The products were lyophilized and characterized by SELDI-TOF mass spectrometry. The concentration of constructs was determined by absorbance using the following molar extinction coefficients: ε_{556}=104,000 $M^{-1}\cdot cm^{-1}$ (for Alexa546-pHLIPs), ε_{650}=239,000 $M^{-1}\cdot cm^{-1}$ (for Alexa647-pHLIPs), ε_{753}=290,000 $M^{-1}\cdot cm^{-1}$ (for Alexa750-pHLIPs), ε_{673}=209,000 $M^{-1}\cdot cm^{-1}$ (for Cy5.5-pHLIPs), ε_{672}=165,000 $M^{-1}\cdot cm^{-1}$ (for IR680-pHLIPs), ε_{778}=300,000 $M^{-1}\cdot cm^{-1}$ (for IR800-pHLIPs), ε_{684}=140,000 $M^{-1}\cdot cm^{-1}$ (for Dy680-pHLIPs) and ε_{684}=180,000 $M^{-1}\cdot cm^{-1}$ (for DyP680-pHLIPs).

Absorbance and fluorescence measurements

Absorbance and fluorescence measurements were carried out on a Genesys 10S UV-Vis (Thermo Scientific) spectrophotometer and a SpectraMax M2 (Molecular Devices) spectrofluorometer, respectively. The excitation wavelengths were the following for different constructs: 550 nm for Alexa546-pHLIPs; 650 nm for Alexa647-pHLIPs, 673 nm for Cy5.5-pHLIPs; 680 nm for IR680-pHLIPs, Dy680-pHLIPs and DyP680-pHLIPs; 750 nm for Alexa750-pHLIPs and 780 nm for IR800-pHLIPs.

Cell lines

The 4T1 and 4T1-GFP mouse mammary tumor cell lines were obtained from the American Type Culture Collection and cultured in RPMI medium supplemented with 10% fetal bovine serum, 10 μg/mL of ciprofloxacin in a humidified atmosphere of 5% CO_2 and 95% air at 37°C.

Tumor mouse models

Mammary tumors were established by subcutaneous injection of 4T1 cells ($8x10^5$ cells/0.1 ml/flank) in the right flank of adult female BALB/c mice (about 20 g weight) obtained from Harlan Laboratories. For the metastatic tumor model, 10^6 4T1-GFP cells/50 μl were injected subcutaneously in the mammary fat pad. After approximately 3 weeks, the primary tumor metastasized in the lungs. All animal studies were conducted according to the animal protocol AN04-12-011 approved by the Institutional Animal Care and Use Committee at the University of Rhode Island, in compliance with the principles and procedures outlined by NIH for the Care and Use of Animals.

Fluorescent imaging of organs and tissue

When tumors reached approximately 5-6 mm in diameter tail vein injections of 100 μL of 40 μM of fluorescent pHLIP® peptides were performed. Animals were euthanized at 2, 4, 24 and 48 hours post-injection, and necropsy was performed immediately after euthanization. Tumors and major organs of BALB/c mice were collected for imaging on a FX Kodak in-vivo image station. Fluorescence intensity was obtained via analysis of images by using Kodak software. The contrast index (CI) was calculated according to the equation:

$$CI = \frac{F_{tumor} - F_{backg}}{F_{muscle} - F_{backg}}$$

where F_{tumor} , F_{muscle} and F_{backg} are the mean fluorescence intensities of tumor, muscle and background signal of the same organ from untreated mice, respectively. Fluorescent images of metastatic lesions in lungs were acquired at 4 and 10x magnification using an Olympus IX71 inverted fluorescence microscope.

Multivariate Statistical Analysis

Statistical agglomerative hierarchical clustering algorithm was applied to the database of 24 objects comprising from 3 different pHLIP® variants (WT, Var3, and Var7) conjugated with 8 fluorescent dyes, namely Alexa546 (Al546), Alexa647 (Al647), Alexa750 (Al750), Cy5.5 (Cy5), IR680 (IR680), IR800 (IR800), DyL680 (Dy680) and DyL680-4xPEG (DyP680), measured at time points of 2 and 4 hours. The normalized fluorescent parameters measured in tumor (NFT – normalized fluorescence in tumor), muscle (NFM – normalized fluorescence in muscle), kidney (NFK – normalized fluorescence in kidney), and liver (NFL – normalized fluorescence in liver) and averaged over a number of mice tested per experiment were used in analysis. The Euclidean metric was employed to compute distances and Ward's minimum within-cluster variance criterion was applied as an amalgamation (linkage) rule. The results are presented in a form of hierarchical tree, or dendrogram, with height scaled to percentage for convenience of interpretation. The calculations were performed using the hclust function in R.

Multivariate linear regression analysis was applied on a combined (not averaged) response of four fluorescent variables represented by NFT, NFM, NFL and NFK, and three categorical predictors represented by Time (2, 4 and 24 hours), Dye (8 various fluorescent dyes), and pHLIP® variants (Var3, Var7, and WT). The maximum-likelihood method was used to estimate a matrix of regression coefficients, which in the multivariate linear model is equivalent to equation-by-equation least squares estimation for the individual responses. Commonly employed multivariate analysis of variance (MANOVA) procedures such as Pillai-Bartlett Trace, Hotelling-Lawley Trace, and Wilks's Lambda [15] were used to take into account correlation in

four fluorescent variables and to check overall statistical significance of three categorical predictors. The calculations were performed using the lm and manova functions in R.

RESULTS

The focus of our work was targeting of mammary tumors by three pHLIP® variants recently selected for pre-clinical development [7, 9, 13]:

WT: ACEQNPIYWARYADWLFTTPLLLLDLALLVDADEGT

Var3: ACDDQNPWRAYLDLLFPTDTLLLDLLW

Var7: ACEEQNPWARYLEWLFPTETLLLEL

Each peptide had a single Cys residue at the N-terminus for conjugation with fluorescent dyes. We used fluorophores emitting at visible and near-infrared wavelengths: Alexa546, Alexa647, Alexa750, Cy5.5, Dy680, DyP680, IR680, IR800 (see Table 1). The molecular weights and HPLC retention times, reflecting the hydrophobicity of the investigated fluorescent constructs, are also given in Table 1. The absorption and emission spectra of fluorescent constructs are shown in Supplementary Figure S1. The fluorescence was measured in absence and presence of POPC liposomes to mimic behavior of the fluorescent constructs in membrane-unbound and membrane-bound forms. .

With the selected fluorescent dye, Alexa750, we also investigated performance of the following pHLIP® sequences, where the N-terminal end of the peptides contains six negatively-charged Asp residues for the enhancement of constructs solubility:

Var3M: ACDDDDDDPWQAYLDLLFPTDTLLLDLLW

Var7M: ACDDDDDDPWQAYLDLFPTDTLALDLW

In addition, we studied biodistribution of the constructs, where Alexa546 and Cy5.5 fluorescent dyes were attached to the single Cys residue at the membrane-inserting C-terminus of the Var3 pHLIP® peptide:

Var3-C: ADDQNPWRAYLDLLFPTDTLLLDLLCW

To test tumor targeting by fluorescent pHLIP® peptides we selected the highly tumorigenic and invasive 4T1 mammary carcinoma model, which mimics stage IV of human breast cancer [16-18], and is known to be acidic [19] and targeted very well by pHLIP® peptides [14]. This transplantable cancer cell line can spontaneously metastasize from the primary tumor in the mammary gland to multiple distant sites [20-21]. Fluorescent pHLIP® peptides were administrated intravenously and at different time points ranging from 2 to 48 hours, animals were euthanized, tumor, kidney, liver and muscle were collected and imaged immediately. The representative fluorescent images of tissue and organs obtained at 4 hours after the constructs administration are shown on Figure 1. Very good tumor targeting was observed by all fluorescent pHLIP® peptides .The fluorescent images obtained at different time points were used to calculate changes of the mean surface fluorescence intensity in tissue and organs (Figure 2 and Supplementary Table S1), tumor to organ ratios (Figure 3 and Supplementary Table S2) and contrast index (CI) (Figures 4 and Supplementary Table S3).

Different fluorescent pHLIP® peptides demonstrate different kinetic profiles (Figure 2 and Supplementary Table S1). The highest tumor targeting was observed at 2 or 4 hours post-injection with subsequent decay of the signal. Most fluorescent pHLIP® peptides have low liver accumulation except of Cy5.5-pHLIPs, which are the most hydrophobic construct among the

investigated. We also performed study with Cy7.5-Var3, which is even more hydrophobic, and observed significant liver accumulation (data not shown). Surprisingly, Alexa546 pHLIP® peptides, which are second the most hydrophobic constructs after Cy5.5 pHLIP® peptides, showed very low liver, kidney and muscle accumulation with the highest tumor targeting. Tumor to muscle ratio for Alexa546-Var3 was increasing from ~ 5 to 9 within 24 hrs (Figure 3 and Supplementary Table S2). With the shift to near infrared (NIR) wavelengths of excitation and emission for Alexa647, IR680 and Dy680 pHLIP® peptides higher signal in kidney was monitored. Alexa750 and IR800 pHLIP® peptides demonstrate the highest signal in the kidney and liver. We compared performance of Dy680 and its pegylated version, DyP680. The DyP680 pHLIP® peptides are more polar compared to Dy680 pHLIP® peptides. The most noticeable difference was observed in targeting of the kidney: DyP680 pHLIP® peptides demonstrate about twice higher accumulation in the kidney than Dy680 pHLIP® peptides, which could be related to the renal clearance. In overall the contrast index was enhanced for pegylated versions of the constructs compared to non-pegylated counterparts (Figure 4 and Supplementary Table S3).

The contrast index was calculated only for two time points, 2 and 4 hours, since fluorescent signal in muscle at 24 and 48 hrs post-injection was at the level of the background fluorescence (Figure 4 and Supplementary Table S3). We did not observe any significant difference in CI between various pHLIP® sequences, except of Alexa546-Var3, which showed statistically significant higher CI compared to Alexa546-WT and – Var7. The highest contrast (around 6) was observed for Alexa546-, Dy680- and DyP680 at 2 hrs post-injection. At 4 hrs the highest contrast of >8 was found for Cy5.5 pHLIP® peptides. The lowest CI was detected for IR680 pHLIP® peptides.

We tested ability of pHLIP® peptides to deliver imaging agents into the cell by conjugating Alexa546 and Cy5.5 dyes to the C-terminal part of Var3 of pHLIP® peptide, which inserts into the lipid bilayer of membrane. We selected the most hydrophobic dyes to avoid complications with their translocation across cellular membrane. Our data indicate that CI was very similar for the constructs, where Alexa546 or Cy5.5 dyes were conjugated to the N- or C-terminus. We can conclude that Var3 pHLIP® peptide is capable of delivering of imaging agents not only to the cell surface but also across membrane into a cell. However, the polarity of imaging agent will affect the process of its cellular delivery. Also, we evaluated performance of modified Var3M and Var7M, where several Asp residues were added to the N-terminus of the peptides. The statistically significant improvement was observed only for Alexa750-Var7M compared to Alexa750-Var7.

To evaluate similarities and differences between investigated constructs we applied statistical agglomerative hierarchical clustering (tree-clustering) algorithm to the database of 24 objects comprising four normalized fluorescence parameters (NFT, NFM, NFL, NFK) obtained on 3 different pHLIP® variants conjugated with 8 fluorescent dyes and measured at time points of 2 and 4 hours. The purpose of the algorithm is to build a tree-based hierarchical clustering solution, or dendrogram, to illustrate the similarities between the constructs and the order at which they merge into clusters. The dendrograms for 2 and 4 hours time points were constructed by joining of objects into clusters by using Euclidian measure of distance between objects in the multi-dimensional space of analyzed fluorescent parameters, and then applying an amalgamation Ward's (linkage) rule [22] (Figure 5). The dendrogram height, which reflects the level of

dissimilarity of clusters, was scaled to percentage for convenience of interpretation. The constructs merged at the lower levels of height are more similar in terms of fluorescent parameters than those merged at the higher levels. Significant changes in height in the dendrogram may indicate the data partition into appropriate number of clusters. We chose clustering algorithm because it does not require any a priori assumption about data distribution and allows us to reveal naturally existing classes and quantitatively estimate degrees of their distinctions, oppose to commonly used k-means or model-based clustering hierarchical approaches, which require a pre-defined number of classes. Our analysis allowed to reveal two main clusters, one is containing pHLIP® peptides labeled with NIR dyes (Alexa750 and IR800) and Cy5.5 dye. The other cluster includes pHLIP® peptides labeled with Alexa546, Alexa647, Dy680 and DyP680 fluorescent dyes. It was very clear separation of the cluster containing three pHLIP® variants conjugated to Cy5.5 from the cluster of pHLIP® peptides labeled with NIR dyes.

We also performed multivariate linear regression analysis on a combined (not averaged) response of four fluorescent variables represented by NFT, NFM, NFL and NFK, and three categorical predictors represented by Time (2, 4 and 24 hours), Dye (8 various fluorescent dyes), and pHLIP® sequences (Var3, Var7, and WT). Unlike linear regression performed on each fluorescence parameter separately, multivariate regression takes into account natural correlation between all four parameters. Model coefficients are summarized in Table 2. All coefficients marked by bold color indicate significant difference from corresponding reference levels. The obtained data indicate that the fluorescent signal in tumors and kidneys drops significantly only at 24 hours after constructs administration, while fluorescence in muscle and liver changes over

all period of time (4 and 24 hrs). The most significant difference in tumor and organs targeting is observed for Cy5.5 pHLIP® conjugates. Another group of constructs, which have altered accumulations in organs, consists of the NIR (IR680, IR800 and Al750) pHLIP® peptides. These data are in very good agreement with the results of cluster analysis. Finally, fluorescent Var7 and WT pHLIP® constructs demonstrate statistically significant reduction in tumor targeting compared to fluorescent Var3 pHLIP® constructs.

The Alexa546-Var3 construct was selected for testing of targeting of submillimeter metastatic lesions in lungs. Since 4T1 cells implanted into mice have stable expression of GFP the lesions were identified by GFP fluorescence on the excised fresh lungs tissue by fluorescence microscopy (Figure 6). The GFP signal has excellent co-localization with the Alexa546-Var3 fluorescent indicating that 400-600 μm sized metastatic lesions are acidic and targeted by fluorescent pHLIP® peptide.

DISCUSSION

The approach for targeting of tumors, which we develop, is based on the marking of tumor acidity associated with tumor development, progression, aggressiveness and invasiveness. We have shown previously, that peptides of pHLIP® family deliver optical, PET and SPECT imaging agents to the primary tumors and metastatic lesions in a pH-dependent manner [9, 23-26]. Here we carried out a systematic investigation of targeting of 4T1 mammary tumors, kidney, liver and muscle at different time points after single intravenous administration of various pHLIP® peptides conjugated with eight different fluorescent dyes. Since the most NIR fluorescent dyes are large cyclic molecules (about 1 kDa in mass) they can affect and alter biodistribution of

pHLIP® peptides (about 4 kDa in mass). All fluorescent pHLIP® peptides show slow tumor targeting, which ranged within hours after constructs administration. It is advantageous for drug delivery, since it could enhance pHLIP® peptide-drug circulation in blood. The best tumor targeting was observed for pHLIP® variants (WT, Var3 and Var7) conjugated with Alexa546 at both N- or C-termini of the peptides to tether dye to the membrane of cancer cells in the extracellular or intracellular spaces, respectively. Accumulation of the Alexa546 pHLIP® peptides in other organs and tissue was about 4 times less than in tumor. Thus, Alexa546 potentially can alter biodistribution of pHLIP® peptides in a favorable way, and might be used with pHLIP® peptide-drug conjugates. According to our data, Var3 demonstrates the highest tumor targeting in the most cases. We also showed targeting of submillimeter metastatic lesions in lungs by Alexa546-Var3, which opens opportunity of imaging and treating of metastasis employing pHLIP® technology.

The fluorescent pHLIP® peptides also could have important implication for staining and visualization of cancer cells during surgical procedures [27]. Fluorescence-guided surgery has the promise to improve surgical procedures by determining tumor margins using tumor-specific targeting and by increasing the visual information available to the surgeon [28]. This technique, can possibly lead to complete resection of the tumor tissue with improved survival. On the foundation of the hallmarks of cancer, there is a variety of tumor-specific agents that are available for imaging of cancer [29]. To obtain target-specific fluorescence imaging, the contrast agent has to be sent to the tumor site, and has to be kept by the target while non-bound agents are cleared from the circulation. Mostly, NIR dyes are suited better for tissue staining, since auto fluorescence signal in NIR is much lower compared to visible light. The biodistribution is less

critical, however the highest possible contrast between cancerous and normal tissue is the key. Var3 conjugated either with N- or C-terminus with Alexa546 or Cy5.5 show the highest tumor accumulation and highest contrast between tumor and normal tissue. Among NIR dyes, Alexa750, IR800 or Dy680 and DyP680 might be used for surgical procedures.

ACKNOWLEDGEMENTS. This work was supported by the NIH grant GM073857 to OAA and YKR.

FIGURES LEGENDS

Figure 1. **Distribution of the fluorescent pHLIP® peptides in 4T1 mammary tumors (cut in half), muscle, kidney and liver**. Fluorescent images of tissue and organs were obtained at 4 hrs post-injection (p.i.) after single i.v. administration of WT, Var3 and Var7 peptides conjugated with fluorescent dyes.

Figure 2. Time-dependent distribution of the fluorescent pHLIP® peptides in 4T1 mammary tumors, kidney, liver and muscle quantified by the *ex-vivo* mean fluorescence. The data in each row were normalized to the intensity in tumor of the corresponding fluorescent WT pHLIP® peptide at 2 hours p.i.. The numeric values of non-normalized fluorescent intensities are presented in the Supplementary Table 1.

Figure 3. Tumor to organ ratios calculated for 2, 4 and 24 hrs time points p.i.. The numeric values of tumor to organ ratios are presented in the Supplementary Table 2.

Figure 4. Contrast index (CI) calculated at 2 and 4 hrs time points p.i.. The p-level values were computed based on the two-tailed test, * < 0.05 and ** < 0.005. The red asterisk represent p-level calculated for CI between Dy680-WT and DyP680-WT, Dy680-Var7 and DyP680-Var7. The numeric values of CI are presented in the Supplementary Table 3.

Figure 5. Multivariate statistical analysis. The dendrograms obtained for imaging properties of various fluorescent pHLIP® peptides at 2 and 4 hrs time points p.i.

Figure 6. **Targeting of submillimeter metastatic lesions in lungs**. 4T1-GFP cells were injected subcutaneously in the mammary pad of the mouse. After 3 weeks, the primary tumor metastasized in the lungs. The Alexa546-Var3 was given as a single i.v. tail vein injection. At 4 hrs p.i. animals were euthanized, the lungs were excised and imaged immediately on the fluorescent microscope.

REFERENCES

1. Damaghi M, Wojtkowiak JW, Gillies RJ (2013) pH sensing and regulation in cancer. Front Physiol 4:370.
2. Gerweck LE, Seetharaman K (1996) Cellular pH gradient in tumor versus normal tissue: potential exploitation for the treatment of cancer. Cancer Res 56:1194-1198.
3. Raghunand N, Altbach MI, van Sluis R, et al. (1999) Plasmalemmal pH-gradients in drug-sensitive and drug-resistant MCF-7 human breast carcinoma xenografts measured by 31P magnetic resonance spectroscopy. Biochem Pharmacol 57:309-312.
4. Estrella V, Chen T, Lloyd M, et al. (2013) Acidity generated by the tumor microenvironment drives local invasion. Cancer Res 73:1524-1535.
5. Wojtkowiak JW, Rothberg JM, Kumar V, et al. (2012) Chronic autophagy is a cellular adaptation to tumor acidic pH microenvironments. Cancer Res 72:3938-3947.
6. Andreev OA, Engelman DM, Reshetnyak YK (2010) pH-sensitive membrane peptides (pHLIPs) as a novel class of delivery agents. Mol Membr Biol 27:341-352.
7. Andreev OA, Engelman DM, Reshetnyak YK (2014) Targeting diseased tissues by pHLIP insertion at low cell surface pH. Front Physiol 5:97.
8. Andreev OA, Engelman DM, Reshetnyak YK (2009) Targeting acidic diseased tissue: New technology based on use of the pH (Low) Insertion Peptide (pHLIP). Chim Oggi 27:34-37.
9. Weerakkody D, Moshnikova A, Thakur MS, et al. (2013) Family of pH (low) insertion peptides for tumor targeting. Proc Natl Acad Sci U S A 110:5834-5839.
10. Karabadzhak AG, Weerakkody D, Wijesinghe D, et al. (2012) Modulation of the pHLIP transmembrane helix insertion pathway. Biophys J 102:1846-1855.
11. Andreev OA, Karabadzhak AG, Weerakkody D, Andreev GO, Engelman DM, Reshetnyak YK (2010) pH (low) insertion peptide (pHLIP) inserts across a lipid bilayer as a helix and exits by a different path. Proc Natl Acad Sci U S A 107:4081-4086.
12. Karabadzhak AG, An M, Yao L, et al. (2014) pHLIP-FIRE, a cell insertion-triggered fluorescent probe for imaging tumors demonstrates targeted cargo delivery in vivo. ACS Chem Biol 9:2545-2553.
13. Cruz-Monserrate Z, Roland CL, Deng D, et al. (2014) Targeting pancreatic ductal adenocarcinoma acidic microenvironment. Sci Rep 4:4410.
14. Adochite RC, Moshnikova A, Carlin SD, et al. (2014) Targeting breast tumors with pH (low) insertion peptides. Mol Pharm 11:2896-2905.
15. Fox J, Weisberg S (2011) An R Companion to Applied Regression. Thousand Oaks, CA: Sage.
16. Tao K, Fang M, Alroy J, Sahagian GG (2008) Imagable 4T1 model for the study of late stage breast cancer. BMC Cancer 8:228.
17. Yang J, Mani SA, Donaher JL, et al. (2004) Twist, a master regulator of morphogenesis, plays an essential role in tumor metastasis. Cell 117:927-939.
18. Eckhardt BL, Parker BS, van Laar RK, et al. (2005) Genomic analysis of a spontaneous model of breast cancer metastasis to bone reveals a role for the extracellular matrix. Mol Cancer Res 3:1-13.
19. Serganova I, Rizwan A, Ni X, et al. (2011) Metabolic imaging: a link between lactate dehydrogenase A, lactate, and tumor phenotype. Clin Cancer Res 17:6250-6261.
20. Pulaski BA, Ostrand-Rosenberg S (2001) Mouse 4T1 breast tumor model. Curr Protoc Immunol Chapter 20:Unit 20 22.
21. Yang S, Zhang JJ, Huang XY (2012) Mouse models for tumor metastasis. Methods Mol Biol 928:221-228.
22. Ward JH, Jr. (1963) Hierarchical Grouping to Optimize an Objective Function. Journal of the American Statistical Association 58:236–244.

23. Daumar P, Wanger-Baumann CA, Pillarsetty N, et al. (2012) Efficient (18)F-Labeling of Large 37-Amino-Acid pHLIP Peptide Analogues and Their Biological Evaluation. Bioconjug Chem 23:1557-1566.
24. Tapmeier TT, Moshnikova A, Beech J, et al. (2015) The pH low insertion peptide pHLIP Variant 3 as a novel marker of acidic malignant lesions. Proc Natl Acad Sci U S A 112:9710-9715.
25. Vavere AL, Biddlecombe GB, Spees WM, et al. (2009) A novel technology for the imaging of acidic prostate tumors by positron emission tomography. Cancer Res 69:4510-4516.
26. Macholl S, Morrison MS, Iveson P, et al. (2012) In vivo pH imaging with (99m)Tc-pHLIP. Mol Imaging Biol 14:725-734.
27. Keereweer S, Van Driel PB, Snoeks TJ, et al. (2013) Optical image-guided cancer surgery: challenges and limitations. Clin Cancer Res 19:3745-3754.
28. Keereweer S, Kerrebijn JD, van Driel PB, et al. (2011) Optical image-guided surgery--where do we stand? Mol Imaging Biol 13:199-207.
29. Frangioni JV (2003) In vivo near-infrared fluorescence imaging. Curr Opin Chem Biol 7:626-634.

TABLES

Table 1. Spectral properties (position of maximum of excitation, λ_{ex}, and emission, λ_{em}), molecular weights and HPLC retention times of the fluorescent pHLIP® constructs are shown.

Spectral Properties								
	Al546	**Al647**	**Al750**	**Cy5.5**	**IR680**	**IR800**	**Dy680**	**DyP680**
λ_{ex}, nm	556	650	753	630/673	672	778	680	680
λ_{em}, nm	572	670	778	720	702	797	707	707
Molecular Weights								
WT	5146	5362	5462	4853	5140	5303	5084	5866
Var3	4256	4472	4572	3963	4250	4413	4194	4976
Var7	4100	4316	4416	3807	4094	4257	4038	4820
Var3-C	4313	-	-	4020	-	-	-	-
HPLC Retention Times								
WT	29.2	24.8	25.3	29.4	25.5	25.0	26.2	24.9
Var3	27.6	23.3	23.6	28.4	24.3	23.4	25.0	23.7
Var7	25.7	21.6	22.0	26.9	22.8	21.6	23.9	22.0
Var3-C	27.5	-	-	29.8	-	-	-	-

Table 2. The coefficients obtained using multivariate linear regression on a combined response of four fluorescence variables represented by NFT (normalized fluorescence in tumor), NFM (normalized fluorescence in muscle), NFL (normalized fluorescence in liver) and NFK (normalized fluorescence in kidney), and three categorical predictors represented by Time (2, 4 and 24 hours), Dye (8 various fluorescent dyes), and pHLIP® variants (Var3, Var7, and WT). All coefficients marked by bold color indicate significant difference from corresponding reference level. The intercept values correspond to the averages of four fluorescence variables at the reference levels of the predictors: Time = 2 hours, Dye = Al546, and pHLIP® variant = Var3.

	NFT	**NFM**	**NFL**	**NFK**
Intercept	**1.325**	**0.312**	0.685	0.615
Time				
2h (Reference)	0	0	0	0
4h	0.058	**-0.033**	**-0.178**	-0.101
24h	**-0.548**	**-0.190**	**-0.678**	**-0.615**
Dye				
Al546 (Reference)	0	0	0	0
Al647	0.002	**0.093**	**0.293**	**1.036**
Dy680	**-0.321**	**-0.017**	0.084	0.171
DyP680	**-0.300**	**-0.047**	0.041	**1.132**
IR680	-0.019	0.321	**0.427**	**0.483**
Al750	**-0.178**	0.007	**0.549**	**1.860**
IR800	0.091	**0.087**	**1.147**	**2.274**
Cy5.5	**0.215**	**0.081**	**1.701**	**0.635**
pHLIP® variant				
Var3 (Reference)	0	0	0	0
Var7	**-0.530**	**-0.094**	**-0.380**	**-0.181**
WT	**-0.226**	**-0.029**	-0.074	**-0.178**
Adjusted R-squared	0.6986	0.8127	0.780	0.814

FIGURES

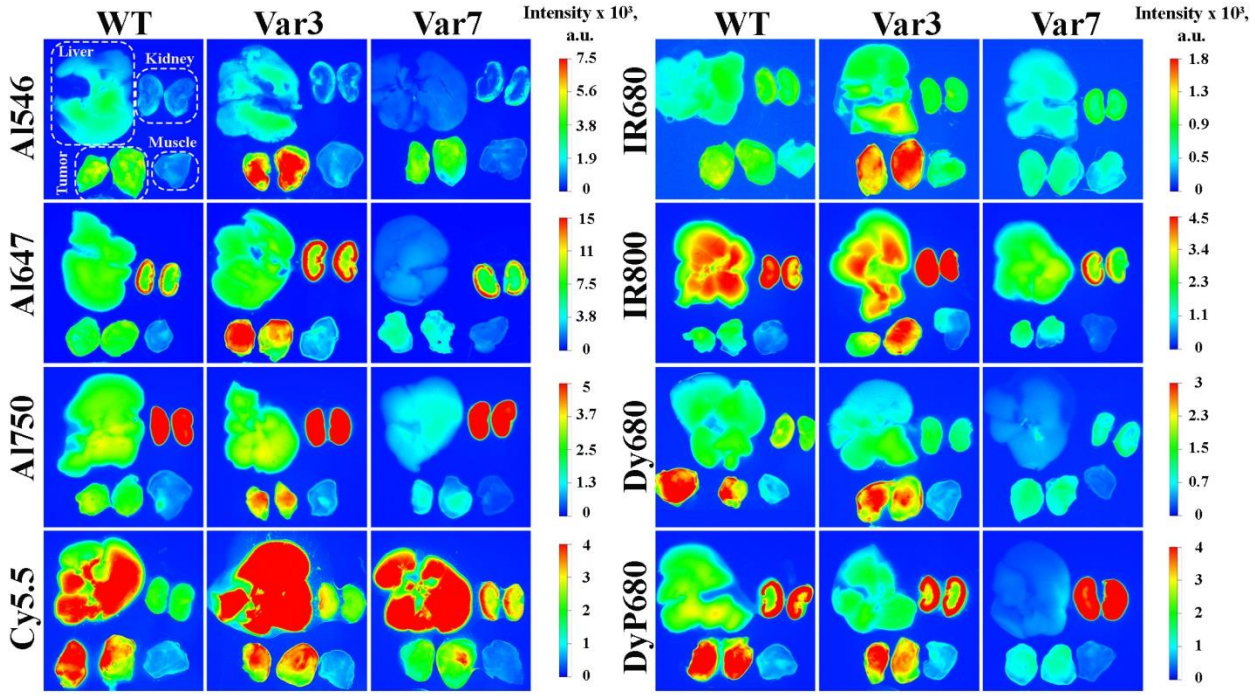

Figure 1

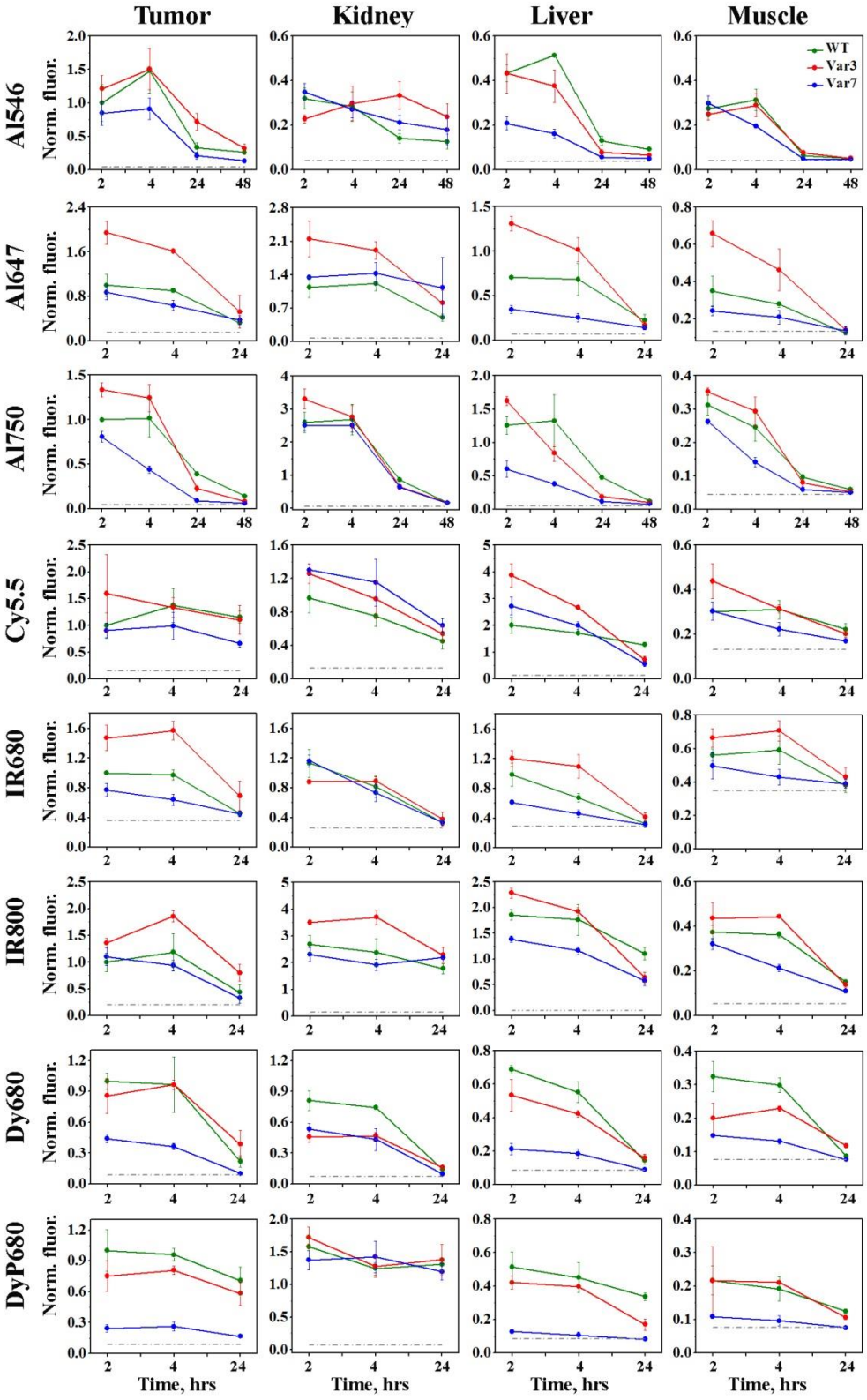
Tumor
Kidney
Liver
Muscle
WT
Var3
Var7
AI546
AI647
AI750
Cy5.5
IR680
IR800
Dy680
DyP680
Norm. fluor.
Time, hrs

Figure 2

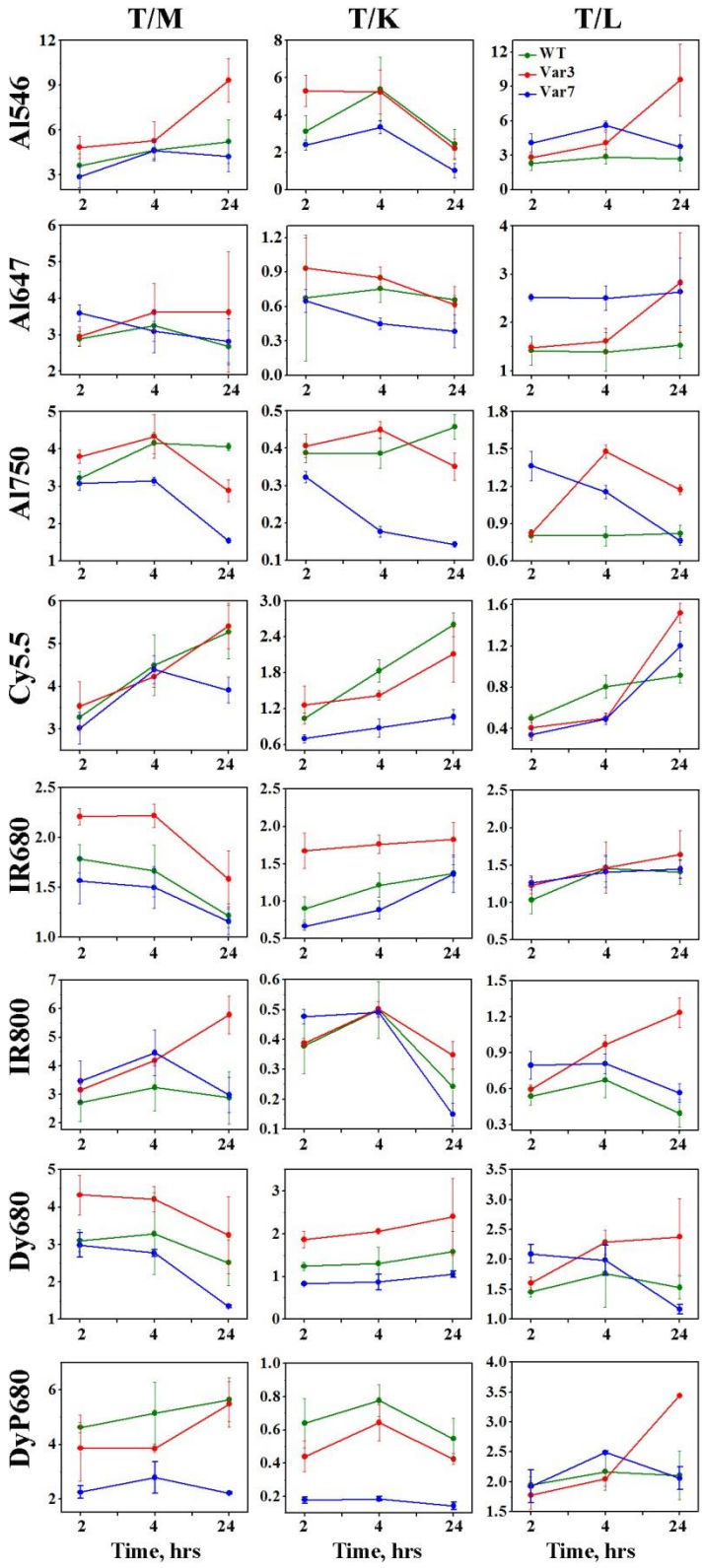
T/M
T/K
T/L
WT
Var3
Var7
Al546
Al647
Al750
Cy5.5
IR680
IR800
Dy680
DyP680
Time, hrs
Time, hrs
Time, hrs

Figure 3

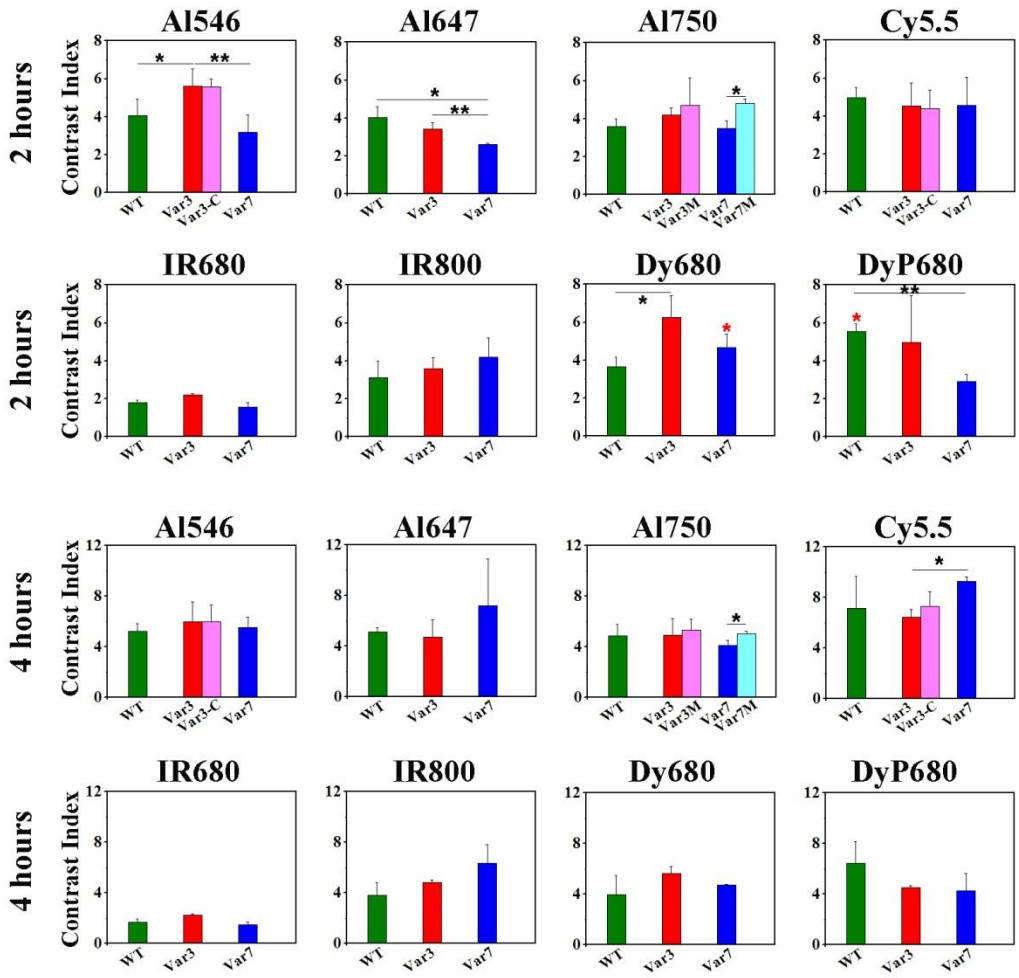
2 hours
4 hours
Contrast Index
Al546
Al647
Al750
Cy5.5
IR680
IR800
Dy680
DyP680
WT
Var3
Var3-C
Var3M
Var7
Var7M

Figure 4

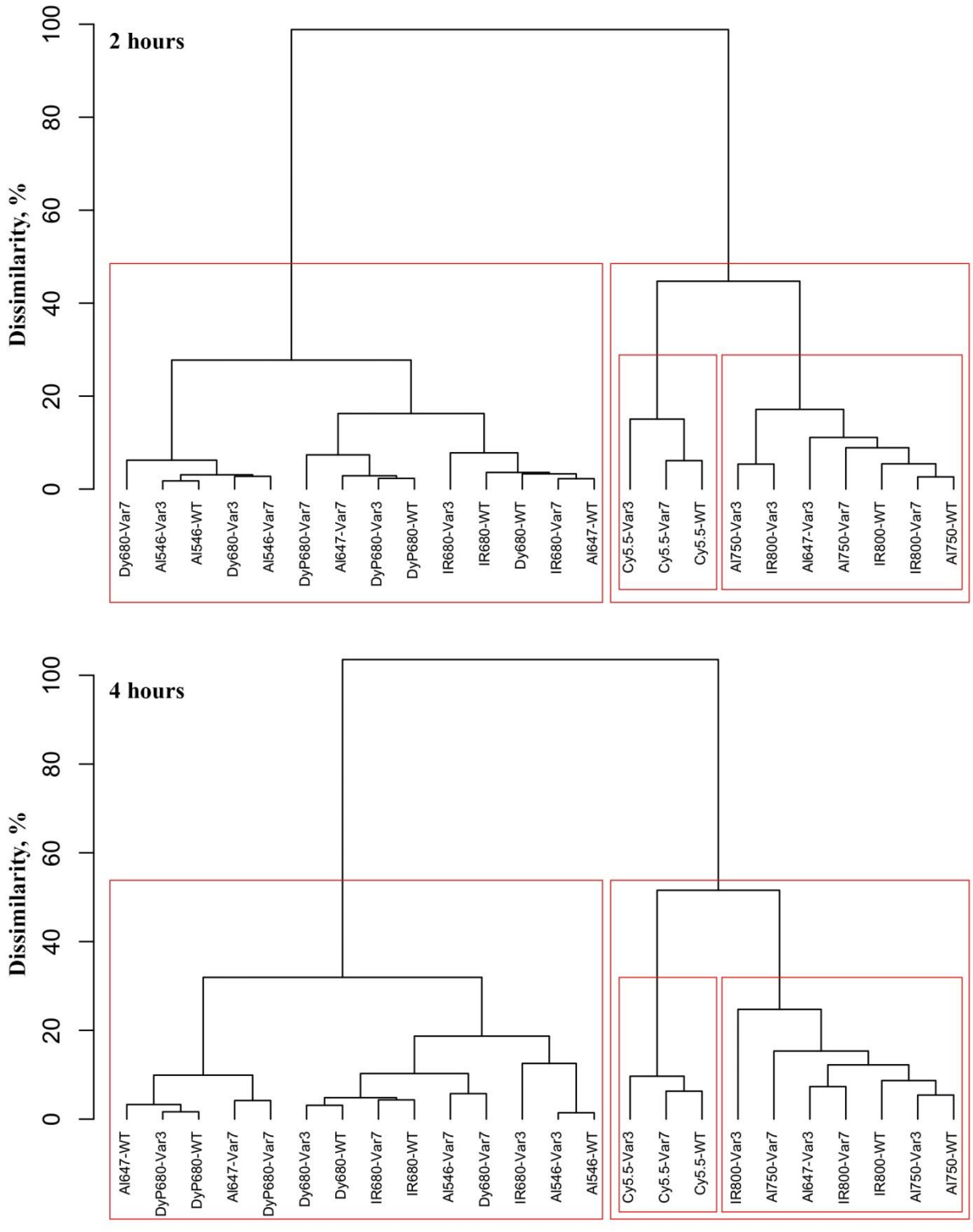
2 hours
Dissimilarity, %
0
20
40
60
80
100
Dy680-Var7
Al546-Var3
Al546-WT
Dy680-Var3
Al546-Var7
DyP680-Var7
Al647-Var7
DyP680-Var3
DyP680-WT
IR680-Var3
IR680-WT
Dy680-WT
IR680-Var7
Al647-WT
Cy5.5-Var3
Cy5.5-Var7
Cy5.5-WT
Al750-Var3
IR800-Var3
Al647-Var3
Al750-Var7
IR800-WT
IR800-Var7
Al750-WT
4 hours
Dissimilarity, %
0
20
40
60
80
100
Al647-WT
DyP680-Var3
DyP680-WT
Al647-Var7
DyP680-Var7
Dy680-Var3
Dy680-WT
IR680-Var7
IR680-WT
Al546-Var7
Dy680-Var7
IR680-Var3
Al546-Var3
Al546-WT
Cy5.5-Var3
Cy5.5-Var7
Cy5.5-WT
IR800-Var3
Al750-Var7
Al647-Var3
IR800-Var7
IR800-WT
Al750-Var3
Al750-WT

Figure 5

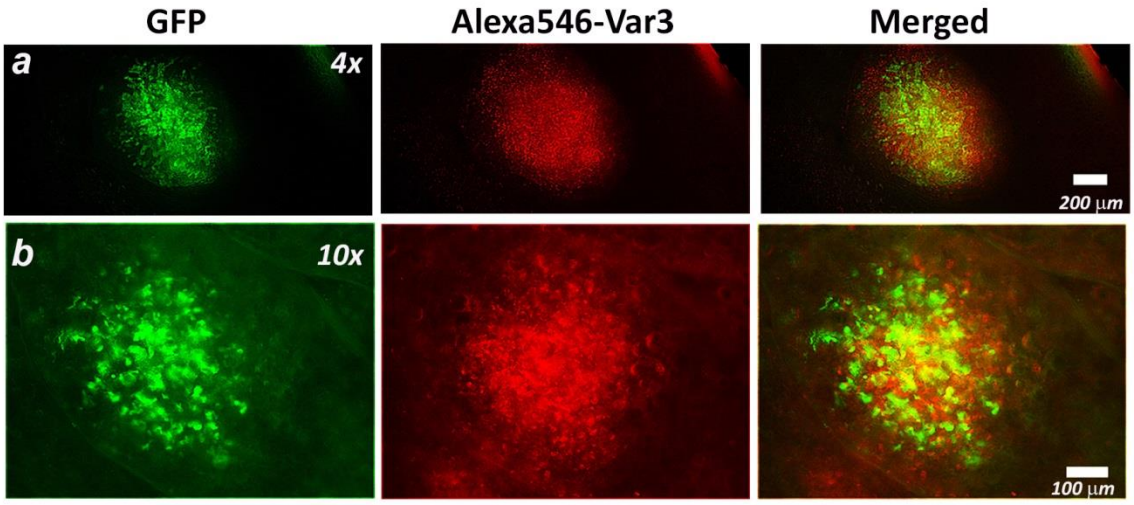

Figure 6

SUPPLEMENTARY MATERIAL

Comparative study of tumor targeting and biodistribution of pH (Low) Insertion Peptides (pHLIP® peptides) conjugated with different fluorescent dyes

Ramona-Cosmina Adochite, Anna Moshnikova, Jovana Golijanin, Oleg A. Andreev, Natallia Katenka, Yana K. Reshetnyak

Table S1. Mean surface fluorescence obtained from the organs and tissue at different time points after single i.v. administration of the fluorescent constructs. Values for the control represent baseline autofluorescence signal from animals with no injection of fluorescent constructs. The number of animals for each time point and each construct is indicated by *n*.

Alexa546-pHLIPs						
Organs	**Time post-injection**	**WT *n*=6**	**Var3 *n*=6**	**Var3-C n=3**	**Var7 *n*=6**	**Control**
Muscle	**2 hrs**	1057.0 ±137.8	963.4 ± 120.8	281.6 ± 23.3	1150.2 ± 126.6	156.3
	4 hrs	1212.0 ± 189.4	1117.9 ± 167.3	283.8 ± 52.6	756.9 ± 34.9	
	24 hrs	249.4 ± 23.2	297.7 ± 28.6	209.5 ± 18.6	191.2 ± 8.34	
	48 hrs	193.6 ± 18.0	201.0 ± 13.3		179.4 ±16.1	
Tumor	**2 hrs**	3856.7 ± 1058.5	4664.5 ± 720.4	834.6 ± 86.6	3267.1 ± 690.0	170.2
	4 hrs	5716.8 ± 1284.8	5809.9 ± 880.4	847.3 ± 162.2	3514.1 ± 622.9	
	24 hrs	1287 ± 290.4	2772.9 ± 600.3	1168.5 ± 299.8	810.4 ± 196.2	
	48 hrs	999.5 ± 129.8	1229.6 ± 281.9		516.7 ± 128.9	
Liver	**2 hrs**	1671.7 ± 148.7	1670.3 ± 409.5	380.3 ± 39.2	805.8 ± 112.4	144.2
	4 hrs	1984.0 ± 27.9	1448.7 ± 317.7	288.4 ± 11.8	623.6 ± 77.2	
	24 hrs	502.5 ± 85.6	303.4 ± 64.4	229.5 ± 17.6	217.0 ± 21.8	
	48 hrs	357.2 ± 24.6	254.9 ± 37.2		193 ± 20.6	
Kidney	**2 hrs**	1235.5 ± 182.2	880.3 ± 51.2	326.8 ± 83.1	1346.8 ± 145.8	156.4
	4 hrs	1099.2 ± 254.3	1148.4 ± 326.7	327.7 ± 41.3	1045.2 ± 144.4	
	24 hrs	544.8 ± 85.9	1288.7 ± 253.3	291.9 ± 17.9	821.3 ± 122.5	
	48 hrs	485.4 ± 126.5	918.5 ± 225.9		690.5 ± 259.6	

Alexa647-pHLIPs					
Organs	**Time post-injection**	**WT *n*=3**	**Var3 *n*=3**	**Var7 *n*=3**	**Control**
Muscle	**2 hrs**	2617.5 ± 616.0	4940.6 ± 527.6	1818.8 ± 200.0	980.7
	4 hrs	2093.2 ± 111.4	3467.6 ± 839.4	1569.0 ± 275.9	
	24 hrs	932.8 ± 49.0	1054.8 ± 121.0	1016.0 ± 171.7	
Tumor	**2 hrs**	7498.5 ± 1480.5	14565.3 ± 1577.3	6556.0 ± 1013.2	1125.5
	4 hrs	6798.8 ± 221.9	12099.6 ±255.7	4781.5 ± 675.1	

	24 hrs	2480.1 ± 290.3	3948.6 ± 2212.7	2832.5 ± 588.2	
Liver	**2 hrs**	5311.2 ± 97.9	9832.4 ± 622.3	2598.1 ± 335.6	525.6
	4 hrs	5137.2 ± 1330.5	7615.7 ± 1028.3	1921.6 ± 351.0	
	24 hrs	1680.4 ± 490.3	1327.4 ± 298.0	1091.4 ± 175.4	
Kidney	**2 hrs**	8516.0 ± 1611.7	16126.9 ± 2787.4	10112.8 ± 391.6	552.6
	4 hrs	9135.8 ± 1167.8	14325.3 ± 1332.3	10696.1 ± 1726.5	
	24 hrs	3778.7 ± 550.7	6081.2 ± 2036.8	8461.9 ± 4773.8	

Alexa750-pHLIPs

Organs	**Time post-injection**	**WT** ***n*=3**	**Var3** ***n*=3**	**Var7** ***n*=3**	**Control**
Muscle	**2 hrs**	889.8 ± 87.2	1002.6 ± 30.7	749.4 ± 21.4	127.3
	4 hrs	700.2 ± 117.8	836.3 ± 123.7	401.0 ± 40.8	
	24 hrs	275.5 ± 10.1	228.0 ± 24.5	169.0 ± 10.8	
	48 hrs	168.7 ± 7.3	150.4 ± 4.2	144.8 ± 0.3	
Tumor	**2 hrs**	2847.7 ± 40.1	3800.4 ± 226.1	2301.2 ± 172.6	135.4
	4 hrs	2897.5 ± 610.4	3542.2 ± 431.8	1256.4 ± 110.8	
	24 hrs	1118.9 ± 76.5	650.9 ± 88.8	260.7 ± 10.3	
	48 hrs	414.6 ± 23.7	236.8 ± 15.7	180.8 ± 16.9	
Liver	**2 hrs**	3577.2 ± 375.5	4618.6 ± 183.6	1722.5 ± 350.7	140.3
	4 hrs	3776.3 ± 1111.3	2401.4 ± 344.5	1087.8 ± 13.4	
	24 hrs	1370.9 ± 104.7	553.2 ± 46.8	342.7 ± 19.3	
	48 hrs	363.1 ± 36.6	286.9 ± 11.6	226.8 ± 21.7	
Kidney	**2 hrs**	7413.1 ± 881.7	9417.1 ± 862.6	7146.2 ± 419.3	143.5
	4 hrs	7664.2 ± 1328.6	7891.6 ± 984.4	7131.0 ± 552.1	
	24 hrs	2459.8 ± 164.2	1869.1 ± 197.4	1836.9 ± 236.7	
	48 hrs	491.2 ± 50.3	487.5 ± 74.6	429.2 ± 16.6	

Alexa750-pHLIP-Mutants

Organs	**Time post-injection**	**Var3M** ***n*=3**	**Var7M** ***n*=3**	**Control**
Muscle	**2 hrs**	886.2 ± 197.3	628.3 ± 24.2	146.9
	4 hrs	774.2 ± 255.2	430.1 ± 47.1	
Tumor	**2 hrs**	3444.6 ± 311.3	2451.8 ± 162.1	144.1
	4 hrs	3355.9 ± 796.2	1562.9 ± 240.4	
Liver	**2 hrs**	3954.1 ± 46.2	1389.4 ± 129.5	144.2
	4 hrs	2313.2 ± 373.7	902.0 ± 79.4	
Kidney	**2 hrs**	9114.2 ± 529.2	9691.2 ± 176.0	146.5
	4 hrs	8615.9 ± 657.4	8275.0 ± 499.0	

Cy5.5-pHLIPs						
Organs	**Time post-injection**	**WT *n*=3**	**Var3 *n*=3**	**Var3-C *n*=3**	**Var7 *n*=3**	**Control**
Muscle	2 hrs	634.1 ± 83.7	918.8 ± 162.6	1035.1 ± 63.4	638.0 ± 86.3	276.1
	4hrs	652.3 ± 88.4	660.5 ± 36.6	719.4 ± 113.4	467.3 ± 63.0	
	24hrs	466.5 ± 54.2	424.2 ± 30.8	411.3 ± 4.4	356.7 ± 16.5	
Tumor	2 hrs	2094.8 ± 497.0	3343.2 ± 1526.1	3627.7 ± 441.5	1900.3 ± 293.5	316.9
	4hrs	2882.6 ± 660.6	2798.5 ± 395.2	3482.0 ± 502.7	2076.3 ± 531.5	
	24hrs	2419.5 ± 226.1	2312.5 ± 556.1	2371.9 ± 186.9	1390.8 ± 141.9	
Liver	2 hrs	4209.2 ± 603.7	8118.0 ± 901.8	7828.1 ± 1161.2	5706.9 ± 719.4	259.5
	4hrs	3587.1 ± 127.3	5589.0 ± 129.6	5916.4 ± 843.6	4177.2 ± 278.0	
	24hrs	2666.9 ± 229.0	1513.1 ± 248.1	1844.5 ± 437.3	1180.8 ± 197.8	
Kidney	2 hrs	2024.9 ± 349.3	2641.0 ± 249.2	2926.5 ± 223.8	2729.3 ± 137.4	263.9
	4hrs	1576.9 ± 253.7	1998.0 ± 485.3	2322.7 ± 335.8	2416.3 ± 588.9	
	24hrs	947.9 ± 198.0	1135.4 ± 193.9	1116.7 ± 28.6	1335.8 ± 174.5	

IR680-pHLIPs					
Organs	**Time post-injection**	**WT *n*=3**	**Var3 *n*=3**	**Var7 *n*=3**	**Control**
Muscle	**2 hrs**	523.3 ± 32.9	619.2 ± 50.7	463.5 ± 73.9	324.1
	4 hrs	551.6 ± 80.0	659.5 ± 56.9	401.0 ± 44.6	
	24 hrs	353.6 ± 37.5	401.9 ± 53.1	363.4 ± 23.2	
Tumor	**2 hrs**	931.9 ± 18.8	1370.8 ± 158.3	718.9 ± 83.5	333.1
	4 hrs	906.3 ± 66.0	1462.7 ± 114.7	597.8 ± 69.8	
	24 hrs	426.7 ± 5.5	645.5 ± 185.8	719.7 ± 34.1	
Liver	**2 hrs**	917.9 ± 144.1	1119.3 ± 97.7	569.2 ± 33.3	270.3
	4 hrs	626.3 ± 52.6	1020.2 ± 150.4	427.7 ± 47.2	
	24 hrs	305.8 ± 35.3	389.4 ± 53.3	291.5 ± 33.0	
Kidney	**2 hrs**	1053.0 ± 171.0	821.8 ± 30.6	1081.4 ± 76.1	241.7
	4 hrs	758.6 ± 137.3	830.5 ± 52.5	682.6 ± 107.8	
	24 hrs	353.6 ± 37.5	352.4 ± 89.0	311.6 ± 34.1	

IR800-pHLIPs					
Organs	**Time post-injection**	**WT *n*=3**	**Var3 *n*=3**	**Var7 *n*=3**	**Control**
Muscle	**2 hrs**	630.6 ± 53.2	736.4 ± 116.0	542.9 ± 43.0	127.3
	4 hrs	612.6 ± 25.1	747.9 ± 10.5	359.1 ± 27.7	
	24 hrs	255.6 ± 19.7	231.6 ± 21.1	185.1 ± 14.6	
Tumor	**2 hrs**	1684.9 ± 292.6	2289.3 ± 146.0	1858.2 ± 271.3	135.4
	4 hrs	1996.4 ± 581.3	3129.0 ± 176.4	1585.9 ± 165.8	
	24 hrs	737.5 ± 241.1	1349.9 ± 267.3	554.9 ± 156.6	
Liver	**2 hrs**	3133.4 ± 179.7	3849.9 ± 164.7	2337.0 ± 107.9	140.3

	4 hrs	2969.8 ± 512.7	3238.8 ± 127.2	1964.7 ± 129.2	
	24 hrs	1863.4 ± 201.1	1089.6 ± 165.0	972.4 ± 149.9	
Kidney	**2 hrs**	4529.1 ± 547.1	5908.6 ± 128.3	3885.1 ± 420.8	143.5
	4 hrs	4015.6 ± 861.0	6235.9 ± 470.1	3238.1 ± 345.6	
	24 hrs	2998.4 ± 314.5	3863.7 ± 478.2	3696.5 ± 114.7	
Dy680-pHLIPs					
Organs	**Time post-injection**	**WT** ***n*=3**	**Var3** ***n*=3**	**Var7** ***n*=3**	**Control**
Muscle	**2 hrs**	754.9 ± 106.3	465.4 ± 103.5	345.6 ± 4.7	172.3
	4 hrs	694.3 ± 50.6	533.2 ± 18.3	305.5 ± 16.4	
	24 hrs	203.6 ± 4.8	274.6 ± 15.8	178.9 ± 9.2	
Tumor	**2 hrs**	2326.0 ± 183.6	1998.2 ± 394.4	1029.3 ± 100.8	219.0
	4 hrs	2246.3 ± 627.8	2243.3 ± 103.9	847.4 ± 73.5	
	24 hrs	511.7 ± 129.3	897.0 ± 314.3	241.1 ± 7.8	
Liver	**2 hrs**	1600.0 ± 60.7	1243.7 ± 218.2	495.5 ± 77.8	210.9
	4 hrs	1284.6 ± 142.6	984.2 ± 47.5	431.2 ± 65.6	
	24 hrs	331.8 ± 46.2	373.0 ± 49.8	207.5 ± 20.6	
Kidney	**2 hrs**	1886.5 ± 227.5	1066.6 ± 119.8	1242.9 ± 119.1	160.2
	4 hrs	1728.6 ± 45.4	1088.9 ± 73.8	1004.5 ± 250.7	
	24 hrs	327.9 ± 29.1	375.4 ± 39.5	229.8 ± 22.6	
DyP680-pHLIPs					
Organs	**Time post-injection**	**WT** ***n*=3**	**Var3** ***n*=3**	**Var7** ***n*=3**	**Control**
Muscle	**2 hrs**	829.6 ± 165.3	828.6 ± 389.7	416.5 ± 22.7	172.3
	4 hrs	735.1 ± 137.6	808.5 ± 14.8	367.0 ± 58.5	
	24 hrs	478.9 ± 24.9	406.4 ± 27.0	291.1 ± 22.2	
Tumor	**2 hrs**	3832.7 ± 769	2883.7 ± 567.7	936.2 ± 132.2	219.0
	4 hrs	3679.4 ± 225.9	3104.6 ± 162.4	1008.8 ± 166.8	
	24 hrs	2716.2 ± 512.0	2239.8 ± 459.6	644.9 ± 60.6	
Liver	**2 hrs**	1968.9 ± 354.6	1614.4 ± 152	488.2 ± 38.9	210.9
	4 hrs	1726.6 ± 343.2	1517.9 ± 26.1	405.6 ± 71.1	
	24 hrs	1290.2 ± 82.3	650.6 ± 131.0	314.1 ± 27.1	
Kidney	**2 hrs**	6047.7 ± 619.5	6584.5 ± 640.1	5262.3 ± 562.0	160.2
	4 hrs	4757.6 ± 360.8	4896.5 ± 656.5	5459.7 ± 928.5	
	24 hrs	5010.1 ± 364.3	5269.3 ± 923.6	4576.4 ± 489.9	

Table S2. Tumor/muscle, tumor/kidney and tumor/liver ratio values.

Ratios	Time post-injection	WT	Var3	Var7
Alexa546-pHLIPs				
Tumor/Muscle	**2 hrs**	3.62 ± 0.77	4.86 ± 0.75	2.89 ± 0.76
	4 hrs	4.68 ± 0.57	5.29 ± 1.27	4.62 ± 0.67
	24 hrs	5.22 ± 1.47	9.32 ± 1.45	4.23 ± 1.00
Tumor/Kidney	**2 hrs**	3.13 ± 0.84	5.30 ± 0.83	2.40 ± 0.26
	4 hrs	5.39 ± 1.70	5.23 ± 1.18	3.36 ± 0.36
	24 hrs	2.45 ± 0.80	2.21 ± 0.52	1.03 ± 0.38
Tumor/Liver	**2 hrs**	2.31 ± 0.60	2.83 ± 0.36	4.09 ± 0.80
	4 hrs	2.88 ± 0.62	4.09 ± 0.98	5.60 ± 0.36
	24 hrs	2.67 ± 1.03	9.57 ± 3.14	3.76 ± 1.02
Alexa647-pHLIPs				
Tumor/Muscle	**2 hrs**	2.88 ± 0.21	2.95 ± 0.26	3.60 ± 0.23
	4 hrs	3.25 ± 0.12	3.61 ± 0.81	3.09 ± 0.58
	24 hrs	2.67 ± 0.44	3.62 ± 1.66	2.81 ± 0.63
Tumor/Kidney	**2 hrs**	0.68 ± 0.55	0.93 ± 0.26	0.65 ± 0.10
	4 hrs	0.75 ± 0.12	0.85 ± 0.09	0.45 ± 0.05
	24 hrs	0.66 ± 0.04	0.62 ± 0.16	0.38 ± 0.14
Tumor/Liver	**2 hrs**	1.42 ± 0.30	1.48 ± 0.09	2.52 ± 0.07
	4 hrs	1.34 ± 0.41	1.61 ± 0.27	2.51 ± 0.25
	24 hrs	1.53 ± 0.28	2.82 ± 1.04	2.64 ± 0.70
Alexa750-pHLIPs				
Tumor/Muscle	**2 hrs**	3.22 ± 0.18	3.80 ± 0.18	3.08 ± 0.18
	4 hrs	4.16 ± 0.29	4.33 ± 0.59	3.14 ± 0.11
	24 hrs	4.06 ± 0.10	2.88 ± 0.30	1.54 ± 0.03
Tumor/Kidney	**2 hrs**	0.39 ± 0.03	0.41 ± 0.03	0.32 ± 0.02
	4 hrs	0.39 ± 0.04	0.45 ± 0.02	0.18 ± 0.01
	24 hrs	0.46 ± 0.03	0.35 ± 0.04	0.14 ± 0.01
Tumor/Liver	**2 hrs**	0.80 ± 0.05	0.82 ± 0.03	1.36 ± 0.12
	4 hrs	0.80 ± 0.08	1.48 ± 0.05	1.15 ± 0.05
	24 hrs	0.82 ± 0.07	1.17 ± 0.04	0.76 ± 0.04
Cy5.5-pHLIPs				
Tumor/Muscle	**2 hrs**	3.28 ± 0.23	3.54 ± 0.57	3.02 ± 0.37
	4 hrs	4.50 ± 0.71	4.23 ± 0.25	4.39 ± 0.32
	24 hrs	5.27 ± 0.63	5.41 ± 0.53	3.91 ± 0.30
Tumor/Kidney	**2 hrs**	1.04 ± 0.09	1.26 ± 0.31	0.70 ± 0.07
	4 hrs	1.83 ± 0.19	1.42 ± 0.08	0.88 ± 0.15
	24 hrs	2.60 ± 0.20	2.11 ± 0.47	1.06 ± 0.13
Tumor/Liver	**2 hrs**	0.50 ± 0.04	0.41 ± 0.09	0.34 ± 0.05
	4 hrs	0.80 ± 0.11	0.50 ± 0.03	0.49 ± 0.06
	24 hrs	0.91 ± 0.07	1.52 ± 0.10	1.20 ± 0.14

IR680-pHLIPs				
Tumor/Muscle	**2 hrs**	1.79 ± 0.14	2.21 ± 0.08	1.57 ± 0.23
	4 hrs	1.67 ± 0.26	2.22 ± 0.12	1.50 ± 0.21
	24 hrs	1.22 ± 0.12	1.58 ± 0.28	1.16 ± 0.13
Tumor/Kidney	**2 hrs**	0.90 ± 0.16	1.67 ± 0.24	0.66 ± 0.06
	4 hrs	1.21 ± 0.17	1.76 ± 0.12	0.89 ± 0.12
	24 hrs	1.37 ± 0.12	1.82 ± 0.23	1.36 ± 0.25
Tumor/Liver	**2 hrs**	1.03 ± 0.19	1.23 ± 0.11	1.26 ± 0.10
	4 hrs	1.46 ± 0.18	1.45 ± 0.34	1.40 ± 0.20
	24 hrs	1.40 ± 0.16	1.64 ± 0.32	1.45 ± 0.12
IR800-pHLIPs				
Tumor/Muscle	**2 hrs**	2.70 ± 0.66	3.15 ± 0.37	3.46 ± 0.72
	4 hrs	3.24 ± 0.82	4.18 ± 0.18	4.45 ± 0.80
	24 hrs	2.88 ± 0.92	5.79 ± 0.67	2.97 ± 0.61
Tumor/Kidney	**2 hrs**	0.38 ± 0.09	0.39 ± 0.02	0.48 ± 0.02
	4 hrs	0.50 ± 0.10	0.50 ± 0.02	0.49 ± 0.02
	24 hrs	0.24 ± 0.06	0.35 ± 0.05	0.15 ± 0.04
Tumor/Liver	**2 hrs**	0.54 ± 0.07	0.59 ± 0.04	0.80 ± 0.11
	4 hrs	0.67 ± 0.15	0.97 ± 0.08	0.80 ± 0.08
	24 hrs	0.39 ± 0.12	1.23 ± 0.12	0.56 ± 0.07
Dy680-pHLIPs				
Tumor/Muscle	**2 hrs**	3.11 ± 0.29	4.32 ± 0.53	2.98 ± 0.33
	4 hrs	3.28 ± 1.09	4.21 ± 0.33	2.77 ± 0.10
	24 hrs	2.51 ± 0.61	3.25 ± 1.02	1.35 ± 0.03
Tumor/Kidney	**2 hrs**	1.24 ± 0.29	1.86 ± 0.20	0.83 ± 0.02
	4 hrs	1.30 ± 0.39	2.06 ± 0.06	0.87 ± 0.18
	24 hrs	1.58 ± 0.48	2.40 ± 0.90	1.05 ± 0.07
Tumor/Liver	**2 hrs**	1.45 ± 0.09	1.60 ± 0.10	2.09 ± 0.15
	4 hrs	1.77 ± 0.56	2.29 ± 0.21	1.99 ± 0.25
	24 hrs	1.53 ± 0.19	2.38 ± 0.64	1.17 ± 0.08
DyP680-pHLIPs				
Tumor/Muscle	**2 hrs**	4.62 ± 0.19	3.86 ± 1.22	2.24 ± 0.23
	4 hrs	5.15 ± 1.14	3.84 ± 0.13	2.78 ± 0.59
	24 hrs	5.65 ± 0.81	5.48 ± 0.84	2.21 ± 0.04
Tumor/Kidney	**2 hrs**	0.64 ± 0.15	0.44 ± 0.09	0.18 ± 0.02
	4 hrs	0.78 ± 0.09	0.64 ± 0.11	0.19 ± 0.01
	24 hrs	0.55 ± 0.12	0.42 ± 0.03	0.14 ± 0.02
Tumor/Liver	**2 hrs**	1.94 ± 0.14	1.78 ± 0.23	1.92 ± 0.27
	4 hrs	2.17 ± 0.31	2.05 ± 0.12	2.49 ± 0.03
	24 hrs	2.11 ± 0.40	3.44 ± 0.02	2.06 ± 0.19

Table S3. Contrast Index (CI) calculated for 2 and 4 hours time points.

Time post-injection	WT	Var3	Var7
Alexa546-pHLIPs			
2 hrs	4.06 ± 0.88	5.60 ± 0.92	3.18 ± 0.90
4 hrs	5.22 ± 0.61	6.01 ± 1.55	5.54 ± 0.81
Alexa647-pHLIPs			
2 hrs	4.03 ± 0.58	3.41 ± 0.35	2.61 ± 0.07
4 hrs	5.12 ± 0.39	4.72 ± 1.39	7.18 ± 3.70
Alexa750-pHLIPs			
2 hrs	3.59 ± 0.40	4.19 ± 0.37	3.49 ± 0.39
4 hrs	4.88 ± 0.92	4.95 ± 1.28	4.13 ± 0.39
Cy5.5-pHLIPs			
2 hrs	4.96 ± 0.56	4.55 ± 1.19	4.58 ± 1.47
4 hrs	7.16 ± 2.54	6.44 ± 0.63	9.27 ± 0.37
IR680-pHLIPs			
2 hrs	1.79 ± 0.14	2.21 ± 0.08	1.57 ± 0.23
4 hrs	1.67 ± 0.26	2.22 ± 0.12	1.50 ± 0.21
IR800-pHLIPs			
2 hrs	3.13 ± 0.87	3.61 ± 0.55	4.21 ± 1.00
4 hrs	3.80 ± 0.10	4.82 ± 0.21	6.37 ± 1.46
Dy680-pHLIPs			
2 hrs	3.67 ± 0.48	6.27 ± 1.13	4.69 ± 0.71
4 hrs	3.97 ± 1.50	5.63 ± 0.56	4.72 ± 0.07
DyP680-pHLIPs			
2 hrs	5.55 ± 0.40	4.99 ± 2.44	2.92 ± 0.36
4 hrs	6.43 ± 1.50	4.53 ± 0.15	4.25 ± 1.40

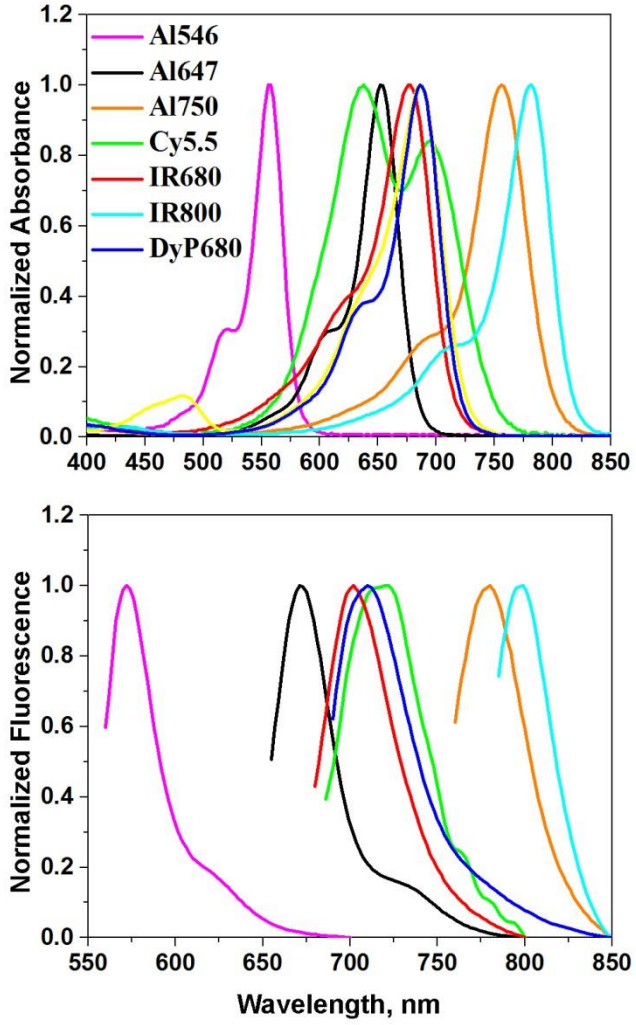

Figure S1. Absorption and fluorescence spectra of fluorescent-constructs measured in PBS.